DMD Fast Forward. Published on March 5, 2012 as doi:10.1124/dmd.111.044362

Metabolic Switching of BILR 355 in the Presence of Ritonavir II: Uncovering Novel Contributions by Gut Bacteria and Aldehyde Oxidase

Yongmei Li, Jun Xu, W. George Lai, Andrea Whitcher-Johnstone and Donald J. Tweedie

Drug Metabolism & Pharmacokinetics, Boehringer Ingelheim Pharmaceuticals, Inc., Ridgefield, CT, USA (Y.L., J.X., W.G.L., A.W., D.J.T.)

DMD Fast Forward. Published on March 5, 2012 as DOI: 10.1124/dmd.111.044362
This article has not been copyedited and formatted. The final version may differ from this version.

RUNNING TITLE: Metabolic Switching of BILR 355 in the Presence of RTV II

Please address correspondence to:

Yongmei Li

Drug Metabolism & Pharmacokinetics

Boehringer Ingelheim Pharmaceuticals, Inc.

900 Ridgebury Rd.,

Ridgefield, CT 06877, USA

Phone: 203-778-7606

Fax: 203-791-6003

E-mail: yongmei.li@boehringer-ingelheim.com

Number of

Text pages: 35

Tables: 2

Figures: 7

References: 27

Number of Words

Abstract: 209

Introduction: 367

Discussion: 1500

Nonstandard Abbreviations**:**

NNRTI, non-nucleoside reverse transcriptase inhibitor; HIV, human immunodeficiency virus; BILR 355, 11-ethyl-5,11-dihydro-5-methyl-8-[2-[(1-oxido-4-quinolinyl)oxy]ethyl]-6H-dipyrido[3,2-b:2',3'-e] [1,4]diazepin-6-one; CYP, cytochrome P450; RTV, ritonavir; DHM, disproportionate human metabolite; HLMs, human liver microsomes; HL, human liver; AO, aldehyde oxidase; LC-MS/MS, high performance liquid chromatography-tandem mass spectrometry; DPBS, Dulbecco's phosphate-buffered saline; *m/z*, mass to charge ratio

ABSTRACT:

Ritonavir (RTV) was used as a boosting agent to increase the clinical exposure of BILR 355, an inhibitor of the human immunodeficiency virus, by inhibiting the CYP3A-mediated metabolism of BILR 355. However, while the levels of BILR 355 increased upon concomitant administration of RTV, a metabolite of BILR 355, BILR 516, which was not detected previously in humans dosed with BILR 355 alone, became a disproportionate human metabolite with levels exceeding the parent levels at steady-state. This was an unusual finding based on *in vitro* and *in vivo* metabolic profiles of BILR 355 available at that time. Our studies reveal that BILR 355 is reduced to an intermediate, BILR 402, by gut bacteria and the reduced metabolite (BILR 402) is then oxidized by aldehyde oxidase to form BILR 516, the disproportionate human metabolite. The role of aldehyde oxidase helped to explain the somewhat unique formation of BILR 516 in humans compared to preclinical animal species. This paper underlines the increasing importance of two individually atypical enzymes in drug development, gut bacterial biotransformation and aldehyde oxidase, which in combination provided a unique metabolic pathway. In addition, this paper clearly elucidates an example of novel metabolic switching and, hopefully, raises awareness of the potential for metabolic switching in combination drug therapies.

DMD Fast Forward. Published on March 5, 2012 as DOI: 10.1124/dmd.111.044362
This article has not been copyedited and formatted. The final version may differ from this version.

Introduction

Non-nucleoside reverse transcriptase inhibitors (NNRTIs) have played an important role in antiretroviral combination regimens for the treatment of the human immunodeficiency virus (HIV)-1 infection, along with nucleoside reverse transcriptase inhibitors, protease inhibitors, fusion inhibitors, CCR5 antagonists, and integrase inhibitors (Klimas et al., 2008). However, the first generation of NNRTIs suffers from a low genetic barrier to resistance (de Béthune, 2010; Thompson et al., 2010). BILR 355 (Fig. 1) is a "second generation" NNRTI which was developed for the treatment of HIV-1 infection in adults and children (Boone, 2006; Bonneau et al., 2005). BILR 355 is highly specific toward HIV-1 reverse transcriptase and exhibits an attractive resistance profile against a broad spectrum of NNRTI-resistant viruses (Bonneau et al., 2005).

BILR 355 has a very short half life (2 to 5 h) and low exposure after oral administration to humans (Huang et al., 2008). *In vitro* metabolism studies suggested that cytochrome P450 (CYP) 3A4 was playing a significant role in limiting systemic exposure to BILR 355 (ref. companion paper). Ritonavir (RTV) is a potent inhibitor of CYP3A that has been used as a boosting agent to increase the exposure of a number of drugs, such as atazanavir and darunavir (Hull and Montaner, 2011). After concomitant administration of BILR 355 with RTV, BILR 355 exposure improved dramatically with AUC increasing 16- to 30-fold (Huang et al., 2008). However, an unexpected consequence of this boosting strategy was that a metabolite, BILR 516 (Fig. 1), which was not detected previously in humans given BILR 355 alone, emerged as a disproportionate human metabolite (DHM) with plasma levels exceeding those of parent at steady-state (Ref. companion paper).

The appearance of BILR 516 as a DHM provided challenges in achieving adequate plasma exposure in preclinical species to cover the human systemic levels. It was therefore of interest to explore how this metabolite was formed. This paper delineates the metabolic pathways for the conversion of BILR 355 to the DHM, BILR 516, and discusses the importance of two individually atypical enzymes in drug development, which in combination provided a unique metabolic pathway. In addition, this paper clearly elucidates the complicated mechanisms of the metabolic switching of BILR 355 upon concomitant administration of the boosting agent, RTV.

DMD Fast Forward. Published on March 5, 2012 as DOI: 10.1124/dmd.111.044362
This article has not been copyedited and formatted. The final version may differ from this version.

Materials and Methods

Chemicals, Reagents and Other Materials. BILR 355, BILR 402, and BILR 516 were synthesized at Boehringer Ingelheim Pharmaceuticals, Inc (Ridgefield, CT) (Fig. 1). BILR 483 (D_3-BILR 355 with three deuterium on the methyl group) and nevirapine were also synthesized at Boehringer Ingelheim Pharmaceuticals, Inc. NADPH was purchased from Sigma-Aldrich (St. Louis, MO). All other reagents and solvents were of analytical grade or higher purity and were obtained from commercial suppliers. Pooled human liver microsomes (HLMs), human liver (HL) cytosol, and HL S9 were obtained from BD Biosciences (Woburn, MA). Individual lots of HLMs (ID # HL081696 and # HL082396B) were prepared in-house. All recombinant CYPs (produced in baculovirus-infected insect cells) and control insect cell microsomes were obtained from BD Biosciences. Cytosolic extract of *Escherichia Coli* expressing recombinant human aldehyde oxidase (AO) and control cytosolic extract of *Escherichia Coli* without recombinant human AO were purchased from Cypex Ltd (Dundee, Scotland, UK). All enzymes were stored at -80 °C until used.

***In Vitro* Incubations.** Incubations were carried out in 0.05 M potassium phosphate buffer, pH 7.4. For incubations with rCYP, HLMs, and HL S9 using NADPH as the cofactor, substrates, inhibitors (when needed), and enzymes were pre-incubated in buffer for 5 minutes at 37 °C and each reaction was initiated with the addition of NADPH at a final concentration of 2.5 mM. For incubations with HL cytosol and S9 in the absence of NADPH, enzymes and inhibitors (when needed) were pre-incubated for 5 minutes at 37°C and each reaction was initiated with the addition of substrate. The final concentrations of enzymes varied and are specified in each study as described below.

DMD Fast Forward. Published on March 5, 2012 as DOI: 10.1124/dmd.111.044362
This article has not been copyedited and formatted. The final version may differ from this version.

The final incubation volume was 0.5 mL or 1 mL and the final organic solvent concentration in each reaction did not exceed 1%. Reactions were carried out for 60 min and at the specified time points, a 50 µL aliquot was transferred to a glass filter plate assembly containing 100 µL of quench solution (0.1 µM nevirapine in acetonitrile or 0.2 µM nevirapine in 40% acetonitrile, 59.9% water and 0.1% acetic acid). The filter plate assembly was centrifuged at 1600 g for 10 min at 4°C. Filtrates from the centrifugation step were analyzed by LC-MS/MS (high performance liquid chromatography- tandem mass spectrometry). Each experiment was performed in duplicate. The general *in vitro* incubation conditions were applied to all assays described below unless specifically stated.

Incubation of BILR 355 with Hepatic Enzymes. BILR 355 at a final concentration of 5 µM was incubated with HLMs, HL cytosol, or HL S9. Protein concentration was 1 mg/mL. The formation of BILR 516 or BILR 402 was monitored at 0, 10, 20, 30 and 60 min by LC-MS/MS.

***In Vitro* Gut Bacteria Incubation**. Individual fecal samples from two healthy male volunteers were collected and transferred to an anaerobic chamber (Coy laboratory products, Inc., Grass Lake, MI). The Coy anaerobic chamber provides a strict anaerobic condition of 0-5 parts per million oxygen atmosphere through a hydrogen gas (5% in nitrogen gas) reacting with a palladium catalyst to remove oxygen. A heavy duty vacuum airlock is connected to the chamber, which allows sample transfer without changes to the internal atmosphere. Dulbecco's phosphate-buffered saline (DPBS) was stirred in the anaerobic chamber overnight to remove oxygen. The fecal samples were mixed with DPBS to obtain a concentration of 0.1 g/mL (weight of fecal sample/volume

of DPBS). The samples were then homogenized and centrifuged at 20 g for 5 min at 4°C to remove debris. The supernatant was diluted to 0.05 g/mL. The samples were transferred to individual wells and pre-incubated for 5 min at 37 ºC. Reactions were initiated by the addition of BILR 355 at a final concentration of 100 µM to each sample. The incubations were performed in duplicate at 37 ºC. Reactions were terminated at 0, 2.5, 5, 7.5, 10, 15, 20, 30, 40, 60, 90, and 120 min and the formation of BILR 402 was measured by LC-MS/MS. All of the *in vitro* steps up to reaction termination were carried out under anaerobic condition.

Incubation of BILR 402 with Hepatic Enzymes. BILR 402, at a final concentration of 10 µM, was incubated with HL S9 or cytosol. Final protein concentration employed in this study was 1 mg/mL. The amount of BILR 516 generated from BILR 402 was measured at 10, 20, 30, and 60 min by LC-MS/MS.

Inhibition of the Biotransformation of BILR 402 to BILR 516 in HL S9 and Cytosol by Enzyme-Selective Inhibitors. To investigate the role of cytosolic enzymes involved in the formation of BILR 516 from BILR 402, BILR 402 (5 µM) was incubated with HL S9 or cytosol at a final protein concentration of 0.5 mg/mL in the presence of various selective inhibitors. The selective chemical inhibitors used in this study were as follows: menadione 50 µM and hydralazine 50 µM for AO, allopurinol 50 µM for xanthine oxidase, disulfiram 50 µM for aldehyde dehydrogenase, and pyrazole 100 µM for alcohol dehydrogenase (Rochat et al., 1998). Controls were performed in the absence of the inhibitors. The incubations were carried out for 60 min and the formation of BILR 516 was measured at 5, 10, 20, 30, and 60 min by LC-MS/MS.

DMD Fast Forward. Published on March 5, 2012 as DOI: 10.1124/dmd.111.044362
This article has not been copyedited and formatted. The final version may differ from this version.

^{18}O Incorporation Assay. BILR 402 was incubated at a final concentration of 5 µM with HL cytosol in 0.05 M potassium phosphate buffer containing 100% $H_2{}^{16}O$ or a mixture of $H_2{}^{16}O$ and $H_2{}^{18}O$ (82:18, v/v). The final protein concentration was 1 mg/mL. The reactions were terminated at 10, 20, 30, and 60 min and the samples were analyzed by LC-MS/MS. The formation of both BILR 516-^{16}O (BILR 516 containing ^{16}O) and BILR 516-^{18}O (BILR 516 containing ^{18}O) were monitored based on LC-MS/MS peak areas.

Incubation with Recombinant AO. BILR 402 was incubated at a final concentration of 5 µM with recombinant human AO or the control cytosol without recombinant human AO. The final protein concentration was 0.1 mg/mL. The formation of BILR 516 at 0, 2, 5, 10, 15, 20, 30, 45, 60 min was measured by LC-MS/MS.

Apparent K_m and V_{max} Determination of the Biotransformation of BILR 402 to BILR 516 in HL Cytosol. To determine kinetic parameters for the biotransformation of BILR 402 to BILR 516 in HL cytosol, BILR 402 was incubated at 12 different concentrations (0.061, 0.122, 0.244, 0.488, 0.977, 1.95, 3.91, 7.81, 15.6, 31.3, 62.5, 125 µM). The incubations were carried out for 10 min at a cytosolic protein concentration of 0.1 mg/mL. These reaction conditions were within the linear range with respect to enzyme content and incubation time. The formation of BILR 516 was monitored by LC-MS/MS.

Apparent K_m and V_{max} Determination of BILR 402 Metabolism: Depletion of BILR 402 and Formation of BILR 355 by HLMs. The apparent K_m and V_{max} values for both BILR 402 depletion and BILR 355 formation in 2 lots of individual HLMs were

determined. Incubations were carried out in 0.1 M potassium phosphate buffer with 5 mM of $MgCl_2$, pH 7.4. The final concentration of HLMs was 0.05 mg/mL and reactions were conducted for 30 min. These reaction conditions were within the linear range with respect to enzyme concentration and incubation time. The initial rates of metabolism were measured at various BILR 402 concentrations (0.05, 0.1, 0.2, 0.5, 1.0, 2.0, 5.0, 10.0, and 20.0 µM). Aliquots (100 µL) were transferred from the incubation mixtures at various time intervals (0.5, 1, 2, 4, 10, 15, 20, and 30 min) and quenched with an equal volume of acetonitrile. Subsequently, 100 µL of BILR 483 (0.2 µM in acetonitrile) was added to each well as the internal standard. All samples were centrifuged at 1600 g for 10 min and both the depletion of BILR 402 and the formation of BILR 355 were monitored by LC-MS/MS.

Metabolism of BI LR 402 by Recombinant CYP Isoforms. BILR 402 (1 or 10 µM) was incubated with recombinant CYP isoforms, including rCYP1A2, rCYP2A6, rCYP2B6, rCYP2C9, rCYP2C19, rCYP2D6, and rCYP3A4, in a 0.1 M potassium phosphate buffer with 5 mM of $MgCl_2$, pH 7.4. The total incubation volume was 900 µL. Control samples were prepared identically, except that microsomal protein from non-transfected insect cells was substituted for individual recombinant CYP isoforms. Aliquots of incubation mixtures were transferred at 0.5, 1, 2, 4, 10, 15, 20, 30 min and quenched with an equal volume of acetonitrile. Subsequently, 100 µL of BILR 483 (0.2 µM in acetonitrile) was added to each well as the internal standard. The plates were centrifuged. The depletion of BILR 402 and the formation of BILR 355 were monitored by LC-MS/MS.

Inhibition of BILR 402 Metabolism in HLMs by Isoform-Selective Inhibitors. BILR 402 (1 µM) was incubated in the presence and absence of isoform selective chemical inhibitors using the same procedure as described in the companion paper (Ref) with the exception that ticlopidine was added as another inhibitor of CYP2C19 at a final concentration of 20 µM and ketoconazole was used as an inhibitor of CYP3A4 only at a final concentration of 3 µM. The final protein concentration was 0.05 mg/mL and the incubation time was 30 min. Both the depletion of BILR 402 and the formation of BILR 355 were monitored by LC-MS/MS.

Equipment and Chromatographic Conditions for *In Vitro* Assays. For apparent K_m and V_{max} determination of BILR 402 metabolism by HLMs and CYP phenotyping studies of BILR 402, concentrations of BILR 355 and BILR 402 were quantitated by an LC-MS/MS system, consisting of a Gilson 215 liquid handler autosampler (Gilson, Inc., Middleton, WI), two Series 200 Micro pumps (Perkin Elmer, Waltham, MA), and a Applied Biosystems MDS Sciex API4000 triple quadrupole mass spectrometer (Applied Biosystems/Sciex, Thornhill, Ontario, Canada). HPLC column used was a Waters Symmetry C_{18} (2 x 50 mm, 3.5 µm particle size, Waters, Milford, MA). Mobile phase compositions were mobile phase A: water/acetonitrile/acetic acid (95:5:0.05 v/v/v) and mobile phase B: water/acetonitrile/acetic acid (5:95:0.05 v/v/v). A 5 min gradient was used, which started at 0% B for 0.2 min, then increased to 100% B in 4.5 min, and maintained at 100% B for 0.2 min before returning to 0% B at a flow rate of 0.25 mL/min. The retention times for BILR 355, BILR 402, and the isotope-labeled internal standard, BILR 483, were 2.7, 2.8, and 2.7 min, respectively. The mass spectrometer was optimized with an IonSpray voltage of 5.5 kV, an ion source temperature of 650 ºC, a

declustering potential at 80 V, and collision energy of 45 V for BILR 402 and 30 V for BILR 355 and BILR 483, respectively. The multiple reaction monitoring transitions requested for BILR 402, BILR 355, and BILR 483 were *m/z* (mass to charge ratio) 426 → 281, *m/z* 442 → 281, and *m/z* 445→ 284, respectively.

Different LC-MS/MS instrumentation was used for other experiments. The system consisted of an SIL-5000 autosampler and two LC-10AD vp pumps (Shimadzu Scientific Instrument, Norwell, MA) connected with a Applied Biosystems MDS Sciex 4000 Q Trap mass spectrometer (Applied Biosystems/Sciex, Thornhill, Ontario, Canada). An Atlantis dC_{18} column (Waters, Milford, MA) was used with the 3.9 × 150 mm dimension and 3 µm particle size. Mobile phases were similar to previously described except that the concentration of acetic acid was 0.1 %. A 5-min gradient with mobile phase B increasing from 45% to 65% was used at a flow rate of 0.7 mL/min. The multiple reaction monitoring transitions requested for BILR 402, BILR 355, BILR 516, BILR 516-^{18}O, and the internal standard nevirapine were *m/z* 426 →281, *m/z* 442 →281, *m/z* 442 →281, *m/z* 444 →281, and *m/z* 267 → 226, respectively and their retention times were 1.9, 2.7, 3.7, 3.7, and 2.4 min, respectively.

Data analysis. The formation rates of BILR 516 from the incubations of BILR 402 with HL cytosol were calculated. The kinetic parameters were determined by non-linear regression analysis using Graph Pad Prism 5 (La Jolla, CA) and fit to a biphasic equation (Tracy, 2006) as shown below.

$$v = \frac{(V_{\max 1} \bullet [S]) + (CL_{\text{int } 2} \bullet [S]^2)}{K_{m1} + [S]}$$

where [S] is substrate concentration, ν is reaction velocity in pmol/min/mg of HL cytosolic protein, V_{max1} is the normalized maximum reaction velocity in pmol/min/mg of HL cytosolic protein and K_{m1} is Michaelis-Menten constant for the high-affinity–low-capacity site (i.e. low K_m and low V_{max}), CL_{int2} is the *in vitro* intrinsic clearance in mL/min/mg of HL cytosolic protein for the second low-affinity but high-capacity site (i.e. high K_m and high V_{max}).

$CL_{int1,\ in\ vitro}$ of BILR 402 metabolism to BILR 516 in cytosol was calculated by V_{max1}/K_{m1}. The following constants were used to estimate $CL_{int1,\ in\ vivo}$ from $CL_{int1,\ in\ vitro}$: a value of 80.7 mg of cytosolic protein/g of liver (Houston and Galetin, 2008), 1800 g of human liver weight, and average 70 kg of human body weight (Davies and Morris, 1993). To calculate the hepatic clearance, the well stirred model was applied and CL_{h1} (mL/min/kg) was calculated using the following equation (Pang and Rowland, 1977):

$$CL_h = \frac{Q_h \times f_u \times CL_{\text{int}}}{Q_h + f_u \times CL_{\text{int}}}$$

Q = hepatic blood flow in human (20.7 mL/min/kg) (Davies and Morris, 1993), fu = fraction of unbound drug (assume fu = 1).

Enzyme kinetics (K_m and V_{max}) of the depletion of BILR 402 and the formation of BILR 355 by HLMs were measured and the clearance ($CL_{int,\ in\ vitro}$ and CL_h) of both processes was calculated using the same procedure as described in the companion paper (Ref).

DMD Fast Forward. Published on March 5, 2012 as DOI: 10.1124/dmd.111.044362
This article has not been copyedited and formatted. The final version may differ from this version.

Results

The DHM BILR 516 is not Generated Directly from BILR 355. BILR 355 was incubated with HLMs, HL S9, or HL cytosol over 60 min at a concentration of 5 μM, which was close to the maximal plasma concentration of BILR 355 in humans (1500 ng/mL, ~ 3.40 μM) at steady state after oral administration of 150 mg BILR 355 and 100 mg RTV twice a day (Huang et al., 2009). No formation of the DHM was observed, suggesting that the DHM is not formed directly from BILR 355.

Formation of the Reduced Metabolite BILR 402 from BILR 355. Based on the structures of BILR 355 and the DHM, it was hypothesized that BILR 355 could go through a two-step metabolic pathway to form the DHM, including reduction of the N-oxide and subsequent oxidation on the carbon adjacent to the heterocyclic nitrogen.

The first step, reduction of N-oxide of BILR 355 to form the reduced metabolite BILR 402 (Fig. 1), can be mediated by liver enzymes or gut bacteria. The formation of the reduced metabolite was then monitored in the incubations of BILR 355 with HLMs, HL S9, and HL cytosol. There was no formation of the reduced metabolite from the parent in these matrices. The possibility of the involvement of gut bacteria in the biotransformation of the parent to the reduced metabolite was tested. Human fecal samples, containing gut bacteria, were obtained from two healthy volunteers and then incubated with BILR 355. The total incubation time was 120 min. Loss of linearity and saturation were observed beyond 15 min. The linear ranges of the formation of the reduced metabolite were plotted (r^2>0.85) for both subjects and shown in Fig. 2.

DMD Fast Forward. Published on March 5, 2012 as DOI: 10.1124/dmd.111.044362
This article has not been copyedited and formatted. The final version may differ from this version.

The second step involved oxidation of the reduced metabolite to the DHM. This possibility was explored in hepatic enzyme systems, including HL S9 and cytosol and the results are shown in Fig. 3. The initial concentration of the reduced metabolite in the incubations was 10 μM. In the absence of NADPH, 59% and 81% of the reduced metabolite were converted to the DHM after 60-min incubations with HL S9 and cytosol, respectively. Interestingly, comparing to what was observed in the absence of NADPH, significantly less of the DHM was generated by HL S9 in the presence of NADPH. The level of the DHM reached about 20% of the starting material at 10 min and leveled off thereafter. Furthermore, based on LC-MS/MS analysis, BILR 355 was generated from the reduced metabolite in the S9 incubations in the presence of NADPH, while BILR 355 was not detected in S9 incubations without NADPH or in the cytosol incubations.

A role for AO in the formation of the DHM from the reduced metabolite was supported by studies using specific chemical inhibitors of major cytosolic enzymes, including menadione and hydralazine for AO, allopurinol for xanthine oxidase, disulfiram for aldehyde dehydrogenase, and pyrazole for alcohol dehydrogenase. The results are shown in Table 1. In the presence of menadione or hydralazine, two specific inhibitors of AO, the formation of the DHM from the reduced metabolite was almost completely abolished. The inhibition effects by other chemical inhibitors were negligible, except that disulfram, a specific inhibitor of aldehyde dehydrogenase, inhibited the reaction more than 50%. However, it has been reported that disulfiram can also inhibit AO (Kitamura et al., 2001). In addition, aldehyde dehydrogenase is known to oxidize only aldehyde to acid, while aldehyde oxidase can catalyze nucleophilic oxidation at an electro-deficient carbon atom in N-heterocycles (e.g. quinoline) (Beedham et al., 2003).

Based on the chemical inhibition results, it is likely that AO is involved in the formation of the DHM from the reduced metabolite.

Water is the source of oxygen in reactions mediated by AO. Water labelled with ^{18}O was added to the incubations of the reduced metabolite with HL cytosol. The LC-MS/MS peaks of BILR 516-^{16}O and BILR 516-^{18}O were monitored and representative LC-MS/MS chromatograms from incubations containing either the mixture of $H_2{}^{16}O$ and $H_2{}^{18}O$ (82:18, v/v) or 100% $H_2{}^{16}O$ (control sample) are presented in Fig. 4. In the LC-MS/MS chromatograms generated from control samples, the peak of BILR 516-^{16}O was predominant, with a very small peak (0.8% of BILR 516-^{16}O based on peak area comparison) shown in the LC-MS/MS transition for BILR 516-^{18}O, which corresponded to the M+2 isotope of BILR 516-^{16}O (Fig. 4A). The LC/MS/MS chromatograms generated from incubations containing the mixture of $H_2{}^{16}O$ and $H_2{}^{18}O$ were different to this control. The BILR 516-^{18}O peak increased significantly compared to the control (Fig 4B). The peak area ratios of BILR 516-^{16}O to BILR 516-^{18}O were 82 to 18 after subtracting the contribution of the M+2 isotope of BILR 516-^{16}O from the peak area of BILR 516-^{18}O across all time points, which was consistent with the ratio of ^{16}O to ^{18}O (82:18) in the starting incubation material. This result confirmed that water was the source for the oxygen incorporated into the DHM, BILR 516, in the incubations of the reduced metabolite with HL cytosol and corroborated the involvement of AO.

Furthermore, the reduced metabolite was incubated with recombinant human AO and the formation of the DHM was clearly observed (Fig. 5). The DHM was not generated in the control cytosol without recombinant human AO.

DMD Fast Forward. Published on March 5, 2012 as DOI: 10.1124/dmd.111.044362
This article has not been copyedited and formatted. The final version may differ from this version.

Kinetic Analysis of the Biotransformation of the Reduced Metabolite BILR 402 to the DHM BILR 516. Apparent K_m and V_{max} parameters for the metabolism of the reduced metabolite to the DHM were determined in HL cytosol. The Eadie-Hofstee plot of the reaction is shown in Fig. 6A and indicated that the kinetics followed a biphasic model. The apparent K_{m1} and V_{max1} values were obtained based on the biphasic model (Fig. 6B). The intrinsic clearance of the high-affinity–low-capacity site, $CL_{int1,\ in\ vitro}$, was calculated to be 437 µL/min/mg of cytosolic protein based on V_{max1}/K_{m1}. Subsequently, $CL_{int1,\ in\ vivo}$ was estimated as 907 mL/min/kg and CL_{h1} was calculated as 20.2 mL/min/kg.

Kinetic Analysis of the Metabolism of the Reduced Metabolite BILR 402 by HLMs. Two lots of pre-characterized HLMs (HL081696 and HL082396B) were selected for the incubations with the reduced metabolite, BILR 402, based on their testosterone 6β-hydroxylase activities (1600 and 3400 pmol/min/mg microsomal protein, respectively) representing a range of low to average CYP3A4 activities from available individual lots of human liver microsomes. The formation of BILR 355 from the reduced metabolite was observed in the incubations. The apparent K_m and V_{max} values for the depletion of the reduced metabolite and the formation of BILR 355 in each lot of HLMs were calculated using non-linear regression analysis based on the Michaelis-Menten equation and the corresponding intrinsic clearance values were derived. The results are summarized in Table 2. The intrinsic clearance of the reduced metabolite ranged from 1.09 to 5.16 mL/min/mg of HLM protein and the intrinsic clearance for the formation of BILR 355 ranged from 0.24 to 0.55 mL/min/mg of HLM protein. The hepatic clearance values for both processes were close to 20 mL/min/kg.

DMD Fast Forward. Published on March 5, 2012 as DOI: 10.1124/dmd.111.044362
This article has not been copyedited and formatted. The final version may differ from this version.

Identification of CYP Isoforms Involved in the Metabolism of the Reduced Metabolite BILR 402. *In vitro* metabolic rates of the depletion of the reduced metabolite and the formation of BILR 355 were measured in incubations of the reduced metabolite (1 and 10 µM) with recombinant CYP 1A2, 2A6, 2B6, 2C9, 2C19, 2D6, and 3A4. Time-dependent depletion of the reduced metabolite was only observed in the incubations with rCYP3A4 in the presence of NADPH. The substrate was depleted from 1 µM starting concentration to 0.25 µM and from 10 µM starting concentration to 5 µM in the first 4 min. In addition, NADPH-dependent formation of BILR 355 from the reduced metabolite was only observed in the incubations with rCYP3A4. The level of BILR 355 initially increased with the incubation time (0.15 µM of BILR 355 was formed by 4 min when the substrate concentration was 1 µM and 0.9 µM of BILR 355 was formed at the same time when the substrate concentration was 10 µM) and then started to decrease. This observation is consistent with the fact that BILR 355 is also a good substrate of CYP3A (Ref. companion paper) and would be further metabolized by CYP3A as the incubation proceeded. The amount of each CYP enzyme used in the incubations was adjusted based on the relative level of each CYP isoform in an average set of human liver microsomes (Shimada et al., 1994). The final concentrations of each CYP isoform were: 1A2: 2 pmol/mL; 2A6: 1 pmol/mL; 2B6: 0.1 pmol/mL; 2C9:1.5 pmol/mL; 2C19: 1.5 pmol/mL; 2D6: 0.3 pmol/mL; 3A4: 5 pmol/mL (calculated based on 0.05 mg/mL of microsomal protein). To bolster this conclusion, the reduced metabolite was also incubated with recombinant CYP isoforms (CYP1A2, CYP2A6, CYP2B6, CYP2C9, CYP2C19, or CYP2D6) at 20-fold higher enzyme levels. No depletion of the reduced metabolite was observed (data not shown). The results confirmed that these

CYP isoforms are not responsible for the overall CYP-mediated metabolism of the reduced metabolite.

In addition, isoform-selective chemical inhibitors of the six major drug metabolizing CYP isoforms were used to investigate the relative contributions of these isoforms to the metabolism of the reduced metabolite. Metabolism of the reduced metabolite by HLMs was monitored as both the depletion of the reduced metabolite and the formation of BILR 355. The results showed that, in the presence of ketoconazole, a selective inhibitor of CYP3A4, 70% of the overall metabolism of the reduced metabolite and 94% of the formation of BILR 355 in HLMs were inhibited. Furafylline, sulfaphenazole, and quinidine as selective inhibitors of CYP1A2, CYP2C9, and CYP2D6, respectively, had no inhibitory effect on the depletion of the reduced metabolite or the formation of BILR 355. Tranylcypromine, at a concentration of 100 μM, inhibited about 30% of the overall metabolism of the reduced metabolite, but had no effect on the formation of BILR 355. Tranylcypromine is an inhibitor of CYP2C19 and CYP2A6 (Dierks et al., 2001). However, another more potent CYP2C19 inhibitor, ticlopidine, did not inhibit the metabolism of the reduced metabolite and as shown above, neither recombinant CYP2C19 nor CYP2A6 catalyzed the metabolism of the reduced metabolite. Although the mechanism of this inhibition is not clear, the data do not support the role of CYP2C19 or CYP2A6 in the metabolism of the reduced metabolite. The current data clearly demonstrate that CYP3A4 is the major enzyme responsible for the CYP-mediated metabolism of the reduced metabolite and the re-generation of BILR 355 by HLMs.

DMD Fast Forward. Published on March 5, 2012 as DOI: 10.1124/dmd.111.044362
This article has not been copyedited and formatted. The final version may differ from this version.

Discussion

Previous studies with BILR 355 had shown that it was extensively metabolized by CYP3A (Ref. companion paper). Concomitant administration of RTV with BILR 355 to inhibit CYP3A and boost the exposure of BILR 355 had the desired effect (Huang et al., 2008). However, a high-level DHM, BILR 516, was observed (Ref: companion paper). Since the DHM had not been previously observed in humans administered BILR 355 alone, it was important to elucidate the metabolic pathway and identify enzymes responsible for the conversion of BILR 355 to the DHM. In this paper, two atypical enzymatic processes were identified, which in combination, provided a unique metabolic pathway. In addition, the metabolic switching of BILR 355 with concomitant administration of RTV was also elucidated.

We first explored potential metabolic mechanisms for the biotransformation of BILR 355 to the DHM. This biotransformation involves reduction of the N-oxide and oxidation on the carbon next to the N-oxide. The likelihood of this biotransformation as a single step reaction is low, which was confirmed by the *in vitro* incubations of BILR 355 with HLMs, HL S9, and HL cytosol, where no formation of the DHM was observed.

Our hypothesis was that this biotransformation is a two-step process with the reduced metabolite, BILR 402, as the intermediate. The first step would be reduction of BILR 355 to BILR 402. Reduction of N-oxide has been shown to occur presystemically or by hepatic enzymes (Sousa et al., 2008; Guengerich, 2001; Kitamura and Tatsumi, 1984a; Kitamura and Tatsumi, 1984b). The second step is the oxidation of BILR 402 at the

DMD Fast Forward. Published on March 5, 2012 as DOI: 10.1124/dmd.111.044362
This article has not been copyedited and formatted. The final version may differ from this version.

carbon next to the nitrogen in the quinoline moiety, which is a typical reaction mediated by AO (Pryde et al., 2010).

The first step was confirmed to be mediated by gut bacteria, since no BILR 402 was formed after incubations of BILR 355 with HLMs, HL S9, and HL cytosol, while extensive formation of BILR 402 was observed in *in vitro* anaerobic incubations with human feces containing gut bacteria. As shown in Fig 2, approximately 8% of BILR 355 was metabolized to the reduced metabolite within 15 min by human feces. This *in vitro* finding is consistent with observations from the ^{14}C ADME animal studies for BILR 355, which indicated that unchanged BILR 355 was present in only trace amounts in feces of mice, rats, and dogs (0-3.3% of the total radioactivity) and the majority of fecal radioactivity could be accounted for by the reduced metabolite and its down-stream metabolites (72.5%-90.4% of the total radioactivity) (Boehringer Ingelheim Pharmaceuticals, Inc., data on file).

The second step is mediated by AO as confirmed with selective chemical inhibitors (Table 1), incorporation of oxygen from H_2O (Fig. 4), and metabolism by recombinant AO (Fig. 5). In addition, the activity was found in the cytosolic subcellular fraction (Over 80% conversion from the reduced metabolite to the DHM by 60 min) and did not require NADPH (Fig. 3A).

The biotransformation of the reduced metabolite to form the DHM followed biphasic kinetics with a low K_{m1} value of 0.772 μM (Fig. 6). The turnover of the reduced metabolite to the DHM is predicted to be high, with a calculated *in vivo* hepatic clearance of 20.2 mL/min/kg which approximates hepatic blood flow in humans (20.7 mL/min/kg),

DMD Fast Forward. Published on March 5, 2012 as DOI: 10.1124/dmd.111.044362
This article has not been copyedited and formatted. The final version may differ from this version.

particularly since *in vitro* data generally under-predicts *in vivo* clearance of AO mediated metabolism (Zientek et al., 2010).

With the combination of two highly efficient metabolic reactions (BILR 355 forms the reduced metabolite which is then further metabolized to the DHM) and the long *in vivo* half-life of the DHM (54.5 h, Ref. companion paper), it is not surprising to see the high exposure of the DHM at steady state in humans.

The reduced metabolite, BILR 402, is the intermediate of the biotransformation from BILR 355 to the DHM. As such, the metabolism of the reduced metabolite was studied. The reduced metabolite was extensively metabolized by CYPs to other products, as demonstrated by high hepatic clearance (> 20 mL/min/kg) of the reduced metabolite (Table 2). When the reduced metabolite was incubated with HL S9, there was substantially less of the DHM formed in the presence of NADPH compared to the absence (Fig. 3B). This could be attributable to extensive metabolism of the reduced metabolite by CYPs in the presence of NADPH, thus minimal substrate was available for AO metabolism at later time points (i.e. beyond 10 min). In addition, it is also possible that the DHM can be further metabolized by CYPs, which could offset the formation of the DHM by AO and result in nearly zero net change of the DHM level after 10 min. The reduced metabolite can also be oxidized back to the parent BILR 355 by CYPs as shown in HLM (11% for HL081696 and 22% for HL082396B of the overall intrinsic clearance of the reduced metabolite; Table 2). CYP3A4 was identified as the major CYP isoform responsible for the metabolism of the reduced metabolite and specifically the formation of BILR 355 based on studies using recombinant CYP isoforms and isoforms-selective inhibitors. Although not tested in these studies, CYP3A5 may also be involved in the

metabolism of BILR 402 and the formation of BILR 355 considering the overlap in substrate specificity between CYP3A4 and CYP3A5. Notably, ketoconazole only inhibited about 70% of HLM-catalyzed metabolism of the reduced metabolite. Thus, it is possible that other liver microsomal enzymes might play a minor role in the metabolism of the reduced metabolite.

The DHM was not detected in the plasma of human subjects administered BILR 355 alone. So why is there such a difference upon addition of RTV? When administered alone, BILR 355 is significantly metabolized by CYP3A to multiple metabolites as illustrated in Fig. 7A. Reduction of BILR 355 by gut bacteria results in the formation of the reduced metabolite BILR 402. The reduced metabolite is also a very good substrate of CYP3A and the absorbed fraction could be extensively metabolized, including oxidation back to BILR 355. Without concomitant administration of RTV, CYP3A-mediated metabolism of BILR 355 and of the reduced metabolite is the predominant metabolic pathways and the formation of the DHM, BILR 516, by AO is negligible. The concomitant administration of RTV with BILR 355 results in the shutdown of the extensive CYP3A-mediated clearance of BILR 355 and of the reduced metabolite (Fig. 7B). BILR 355 levels now increase and, in addition, the absorbed fraction of the reduced metabolite is no longer subject to CYP3A metabolism but is mainly cleared by AO to form the DHM, which is now the predominant pathway. In addition, it is possible that RTV may inhibit the metabolism of BILR 516, which could also cause an increase in BILR 516 exposure.

These studies have clearly elucidated the unusual metabolic pathways of BILR 355 with the involvement of gut bacteria and AO and the novel metabolic switching upon concomitant administration of RTV.

There are 100 trillion microbes resident in a normal human intestine with a higher density in the lower GI tract (Ley et al., 2006). Due to the complexity of drug development, more and more drugs are developed with low solubility, low permeability, or administered with extended release formulations. As such, these drugs will be more likely to reach the lower GI tract, presenting themselves to the host gut bacteria (Sousa et al., 2008). The possible involvement of gut bacteria in the metabolism of drugs needs to be seriously considered.

In addition, AO-mediated metabolism is drawing more and more attention in drug development. Two key areas of concern are the potential for low oral bioavailability of development compounds in humans, resulting from high turnover by AO, and also the marked species differences in AO activity leading to gross species differences in exposure of metabolites formed by AO (Pryde et al., 2010). Generally, high AO activity is observed in human and monkey, followed by hamster, rabbit, guinea pig, rat, and mouse, and AO is deficient in dog (Kitamura et al., 2006; Beedham et al., 1995; Kitamura et al., 2001; Beedham et al., 1987). Since AO activity is generally low or deficient in the standard Toxicology species, a metabolite generated by AO that is major in humans (>10% of the total drug related materials), has a higher chance of being a DHM. BILR 355 metabolism provides a clear example of this issue.

While it was expected from *in vitro* studies (Ref companion paper) that CYP3A would be a major clearance pathway for BILR 355, the extent of metabolic switching upon concomitant administration of RTV was a surprise. Metabolic switching should certainly be considered as more drugs are developed as a combination therapy either to boost the exposure (e.g. HIV protease inhibitors and RTV) or to maximize efficacy with complimentary treatment mechanisms (e.g. combinations of anti-retrovirals with different targets). In addition, this could be more of an issue as a result of potential drug-drug interactions.

This paper underpins the increasing importance of non-P450 drug metabolizing enzymes (e.g. AO and gut bacteria in this case) and, hopefully, raises awareness of potential metabolic switching associated with combination drug therapies.

Acknowledgements:

We thank Yanping Mao, Elsy Philip and Dr. Lin-Zhi Chen for providing the results of the ^{14}C ADME animal studies and thank Dr. Timothy S. Tracy for scientific advice and review of the manuscript.

Authorship Contributions:

Participated in research design: Li, Lai, Tweedie

Conducted experiments: Li, Xu, Lai, Whitcher-Johnstone

Performed data analysis: Li, Xu, Lai,

Wrote or contributed to the writing of the manuscript: Li, Tweedie

DMD Fast Forward. Published on March 5, 2012 as DOI: 10.1124/dmd.111.044362
This article has not been copyedited and formatted. The final version may differ from this version.

References

Beedham C, Bruce SE, Critchley DJ, al-Tayib Y, and Rance DJ (1987) Species variation in hepatic aldehyde oxidase activity. *Eur J Drug Metab Pharmacokinet* **12**:307-310.

Beedham C, Miceli JJ, and Obach RS (2003) Ziprasidone metabolism, aldehyde oxidase, and clinical implications. *J Clin Psychopharmacol* **23**:229-232.

Beedham C, Peet CF, Panoutsopoulos GI, Carter H, and Smith JA (1995) Role of aldehyde oxidase in biogenic amine metabolism. *Prog Brain Res* **106**:345-353.

Bonneau P, Robinson PA, Duan J, Doyon L, Simoneau B, Yoakim C, Garneau M, Bos M, Cordingley M, Brenner B, Spira B, Wainberg M, Huang F, Drda K, Ballow C, Koenen-Bergmann M, and Mayers D (2005) Antiviral characterization and human experience with BILR 355 BS, a novel next-generation non-nucleoside reverse transcriptase inhibitor (NNRTI) with a broad anti HIV-1 profile. 12th Conference on Retroviruses and Opportunistic Infections, Boston, MA.

Boone LR (2006) Next-generation HIV-1 non-nucleoside reverse transcriptase inhibitors. *Curr Opin Investig Drugs* **7**:128-135.

Davies B and Morris T (1993) Physiological parameters in laboratory animals and humans. *Pharm Res* **10**:1093-1095.

de Béthune MP (2010) Non-nucleoside reverse transcriptase inhibitors (NNRTIs), their discovery, development, and use in the treatment of HIV-1 infection: a review of the last 20 years (1989-2009). *Antiviral Res* **85**:75-90.

Dierks EA, Stams KR, Lim HK, Cornelius G, Zhang H, and Ball SE (2001) A method for the simultaneous evaluation of the activities of seven major human drug-metabolizing cytochrome P450s using an in vitro cocktail of probe substrates and fast gradient liquid chromatography tandem mass spectrometry. *Drug Metab Dispos* **29**:23-29.

Guengerich FP (2001) Common and uncommon cytochrome P450 reactions related to metabolism and chemical toxicity. *Chem Res Toxicol* **14**:611-650.

Houston JB and Galetin A (2008) Methods for predicting in vivo pharmacokinetics using data from in vitro assays. *Curr Drug Metab* **9**:940-951.

Huang F, Drda K, Macgregor TR, Scherer J, Rowland L, Nguyen T, Ballow C, Castles M, and Robinson P (2009) Pharmacokinetics of BILR 355 after multiple oral doses coadministered with a low dose of ritonavir. *Antimicrob Agents Chemother* **53**:95-103.

Huang F, Koenen-Bergmann M, Macgregor TR, Ring A, Hattox S, and Robinson P (2008) Pharmacokinetic and safety evaluation of BILR 355, a second-generation nonnucleoside reverse transcriptase inhibitor, in healthy volunteers. *Antimicrob Agents Chemother* **52**:4300-4307.

Hull MW and Montaner JS (2011) Ritonavir-boosted protease inhibitors in HIV therapy. *Ann Med* **43**:375-388.

Kitamura S, Ohashi KNK, Sugihara K, Hosokawa R, Akagawa Y, and Ohta S (2001) Extremely high drug-reductase activity based on aldehyde oxidase in monkey Liver. *Biol Pharm Bull* **24**:856-859.

Kitamura S, Sugihara K, and Ohta S (2006) Drug-metabolizing ability of molybdenum hydroxylases. *Drug Metab Pharmacokinet* **21**:83-98.

Kitamura S and Tatsumi K (1984a) Involvement of liver aldehyde oxidase in the reduction of nicotinamide N-oxide. *Biochem Biophys Res Commun* **120**:602-606.

Kitamura S and Tatsumi K (1984b) Reduction of tertiary amine N-oxides by liver preparations: function of aldehyde oxidase as a major N-oxide reductase. *Biochem Biophys Res Commun* **121**:749-754.

Klimas N, Koneru AO, and Fletcher MA (2008) Overview of HIV. *Psychosom Med* **70**:523-530.

Ley RE, Peterson DA, and Gordon JI (2006) Ecological and evolutionary forces shaping microbial diversity in the human intestine. *Cell* **124**:837-848.

Pang KS and Rowland M (1977) Hepatic clearance of drugs. I. theoretical considerations of a "Well-Stirred" model and a "Parallel Tube" model. influence of hepatic blood flow, plasma and blood cell binding, and the hepatocellular enzymatic activity on hepatic drug clearance. *J Pharmacokinet Biopharm* **5**:625-653.

Pryde DC, Dalvie D, Hu Q, Jones P, Obach RS, and Tran TD (2010) Aldehyde oxidase: an enzyme of emerging importance in drug discovery. *J Med Chem* **53**:8441-8460.

Rochat B, Kosel M, Boss G, Testa B, Gillet M, and Baumann P (1998) Stereoselective biotransformation of the selective serotonin reuptake inhibitor citalopram and its demethylated metabolites by monoamine oxidases in human liver. *Biochemical Pharmacology* **56**:15-23.

Shimada T, Yamazaki H, Mimura M, Inui Y, and Guengerich FP (1994) Interindividual variations in human liver cytochrome P-450 enzymes involved in the oxidation of drugs, carcinogens and toxic chemicals: studies with liver microsomes of 30 Japanese and 30 Caucasians. *J Pharmacol Exp Ther* **270**:414-423.

Sousa T, Paterson R, Moore V, Carlsson A, Abrahamsson B, and Basit AW (2008) The gastrointestinal microbiota as a site for the biotransformation of drugs. *Int J Pharm* **363**:1-25.

Thompson MA, Aberg JA, Cahn P, Montaner JS, Rizzardini G, Telenti A, Gatell JM, Günthard HF, Hammer SM, Hirsch MS, Jacobsen DM, Reiss P, Richman DD, Volberding PA, Yeni P, and Schooley RT; International AIDS Society-USA (2010)

Antiretroviral treatment of adult HIV infection: 2010 recommendations of the international AIDS society-USA panel. *JAMA* **304**:321-333.

Tracy TS (2006) Atypical cytochrome P450 kinetics: implications for drug discovery. *Drugs R D* **7**:349-363.

Zientek M, Jiang Y, Youdim K, and Obach RS (2010) In vitro-in vivo correlation for intrinsic clearance for drugs metabolized by human aldehyde oxidase. *Drug Metab Dispos* **38**:1322-1327.

Footnotes:

This research was funded by Boehringer Ingelheim Pharmaceuticals, Inc.

This work was presented at the 2009 ISSX meeting:

Li Y, Lai G, Xu J, Applegreen A, Tweedie D Metabolic Switching of BILR 355 in the Presence of Ritonavir II: Elucidation of Metabolic Pathway for the Formation of BILR 516. The 16th North American Regional ISSX Meeting, Baltimore, Maryland, October 18 – 22, 2009, #201.

To receive reprint requests:

Yongmei Li

Drug Metabolism & Pharmacokinetics

Boehringer Ingelheim Pharmaceuticals, Inc.

900 Ridgebury Rd.,

Ridgefield, CT 06877, USA

Phone: 203-778-7606

Fax: 203-791-6003

E-mail: yongmei.li@boehringer-ingelheim.com

W. George Lai (Current address: Drug Disposition, Eisai Research Institute, Andover, MA)

Legends for Figures:

FIG. 1. Chemical structures of BILR 355, BILR 402, and BILR 516

FIG. 2. Formation of BILR 402 from the incubations of BILR 355 with human feces (n=2)

FIG. 3. Formation of BILR 516 in incubations of BILR 402 with (A) human liver cytosol in the absence of NADPH and (B) human liver S9 in the absence and presence of NADPH (n=2)

FIG. 4. Incorporation of ^{18}O into BILR 516 in incubations of BILR 402 with HL cytosol in (A) 50 mM phosphate buffer (no $H_2{}^{18}O$) and (B) 50 mM phosphate buffer containing $H_2{}^{18}O$ (final conc. 18%) (n=2)

FIG. 5. Formation of BILR 516 in incubations of BILR 402 with recombinant human AO (n=2)

FIG. 6. Eadie-Hofstee plot (A) and enzyme kinetic curve (B) of the metabolism of BILR 402 to BILR 516 in HL cytosol (n=2)

FIG. 7. (A) Summary of key metabolic pathways of BILR 355 clearance and the formation of BILR 516 (B) metabolic switching in the presence of RTV

DMD Fast Forward. Published on March 5, 2012 as DOI: 10.1124/dmd.111.044362
This article has not been copyedited and formatted. The final version may differ from this version.

Table 1. Effect of inhibitors on the biotransformation of BILR 402 to BILR 516 in HL S9 and cytosol (n=2).

Enzyme	Specific inhibitor	% of activity remaining	
		HL S9	HL cytosol
Control	No inhibitor	100	100
Aldehyde Oxidase	Menadione	14	8
Aldehyde Oxidase	Hydralazine	0	1
Xanthine Oxidase	Allopurinol	91	87
Aldehyde Dehydrogenase	Disulfiram	55	56
Alcohol Dehydrogenase	Pyrazole	103	92

DMD Fast Forward. Published on March 5, 2012 as DOI: 10.1124/dmd.111.044362
This article has not been copyedited and formatted. The final version may differ from this version.

Table 2 Michaelis-Menten kinetic parameters for BILR 402 metabolism and BILR 355 formation in human liver microsomes (n=2).

HLM	HL081696		HL082396B	
CYP3A4 activity (pmol/min/mg)	3400		1600	
	BILR 402 depletion	BILR 355 formation	BILR 402 depletion	BILR 355 formation
Apparent K_m (μM)	0.62	1.74	0.73	0.97
V_{max} (pmol/min/mg of HLM protein)	3199	953	794	231
$CL_{int,\ in\ vitro}$ (mL/min/mg of HLM protein)	5.16	0.55	1.09	0.24
CL_h (mL/min/kg)	20.6	20.0	20.4	19.3

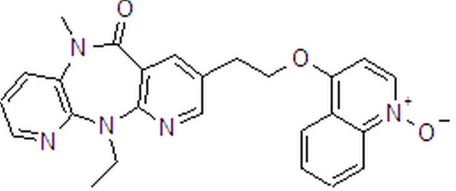

BILR 355

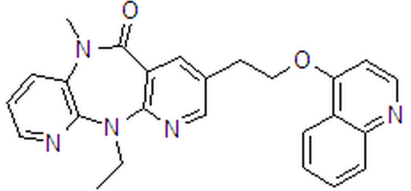

BILR 402

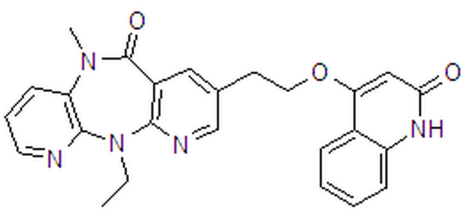

BILR 516

Fig. 1

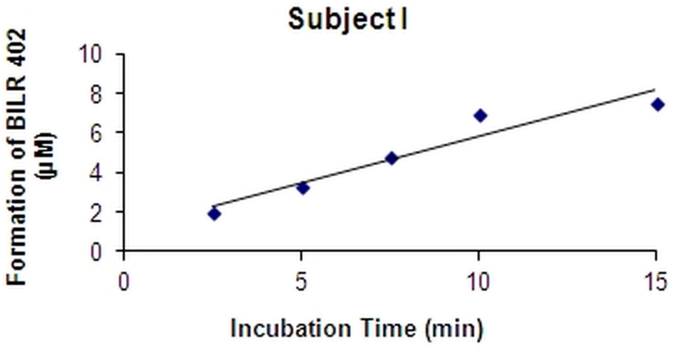
Subject I
Formation of BILR 402 (µM)
10
8
6
4
2
0
0
5
10
15
Incubation Time (min)

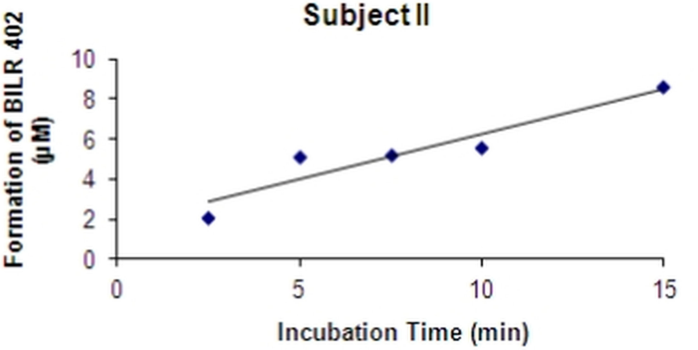
Subject II
Formation of BILR 402 (µM)
10
8
6
4
2
0
0
5
10
15
Incubation Time (min)

Fig. 2

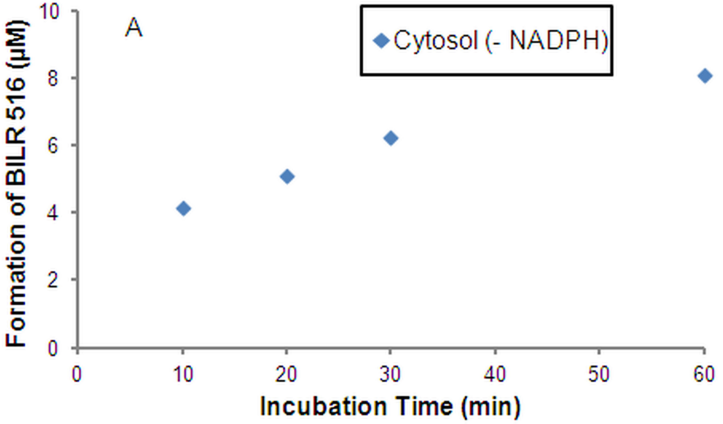
A
Cytosol (- NADPH)
Formation of BILR 516 (µM)
Incubation Time (min)
0
2
4
6
8
10
0
10
20
30
40
50
60

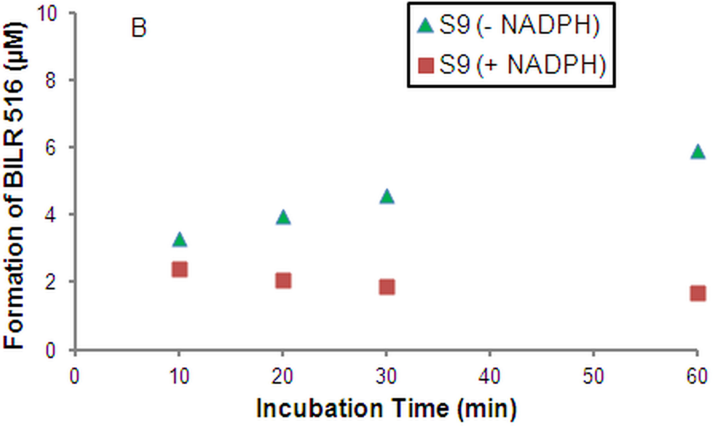
B
S9 (- NADPH)
S9 (+ NADPH)
Formation of BILR 516 (µM)
Incubation Time (min)
0
2
4
6
8
10
0
10
20
30
40
50
60

Fig. 3

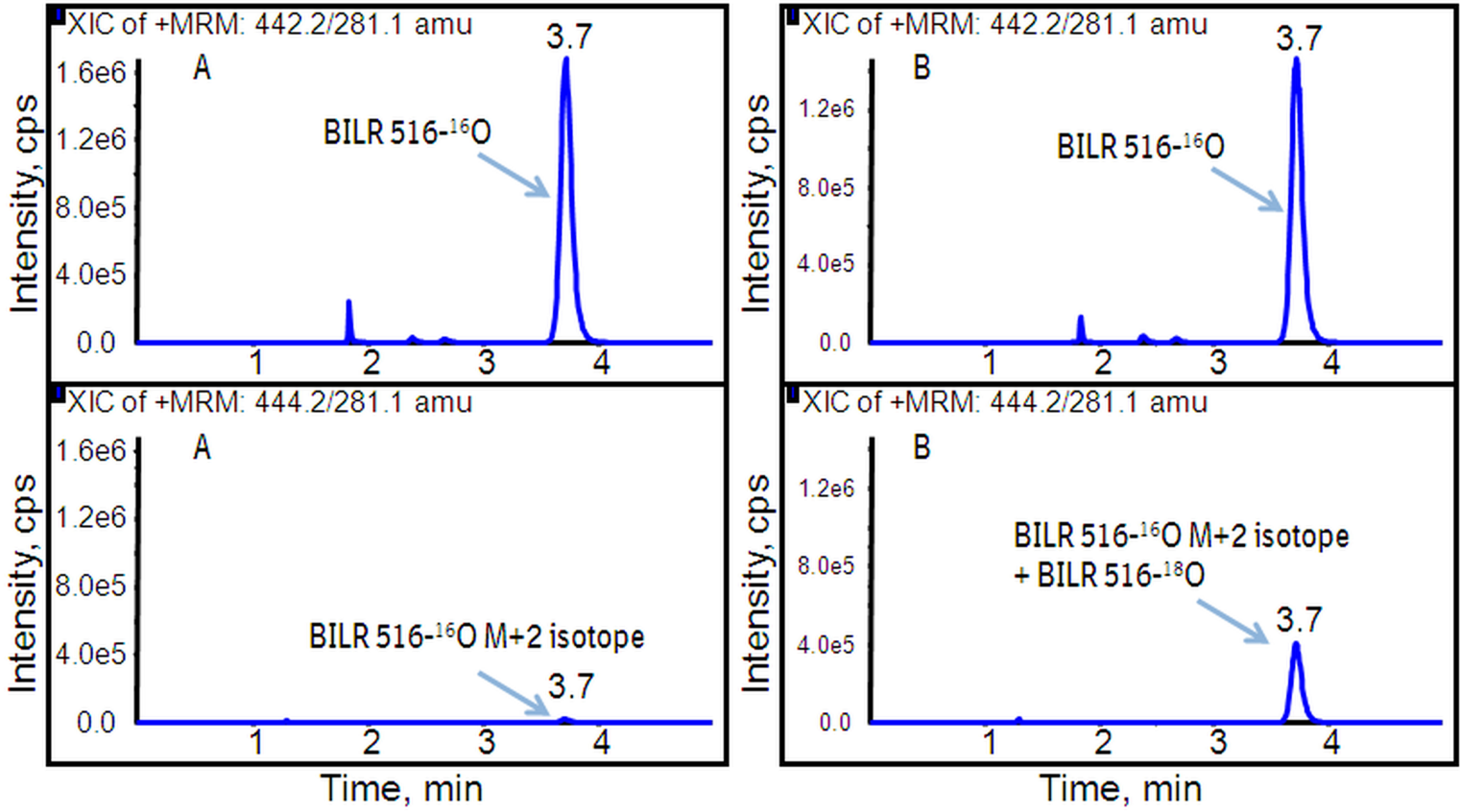
XIC of +MRM: 442.2/281.1 amu
A
3.7
BILR 516-16O
Intensity, cps
1.6e6
1.2e6
8.0e5
4.0e5
0.0
1
2
3
4
XIC of +MRM: 442.2/281.1 amu
B
3.7
BILR 516-16O
Intensity, cps
1.2e6
8.0e5
4.0e5
0.0
XIC of +MRM: 444.2/281.1 amu
A
BILR 516-16O M+2 isotope
3.7
Intensity, cps
Time, min
XIC of +MRM: 444.2/281.1 amu
B
BILR 516-16O M+2 isotope
+ BILR 516-18O
3.7
Intensity, cps
Time, min

Fig. 4

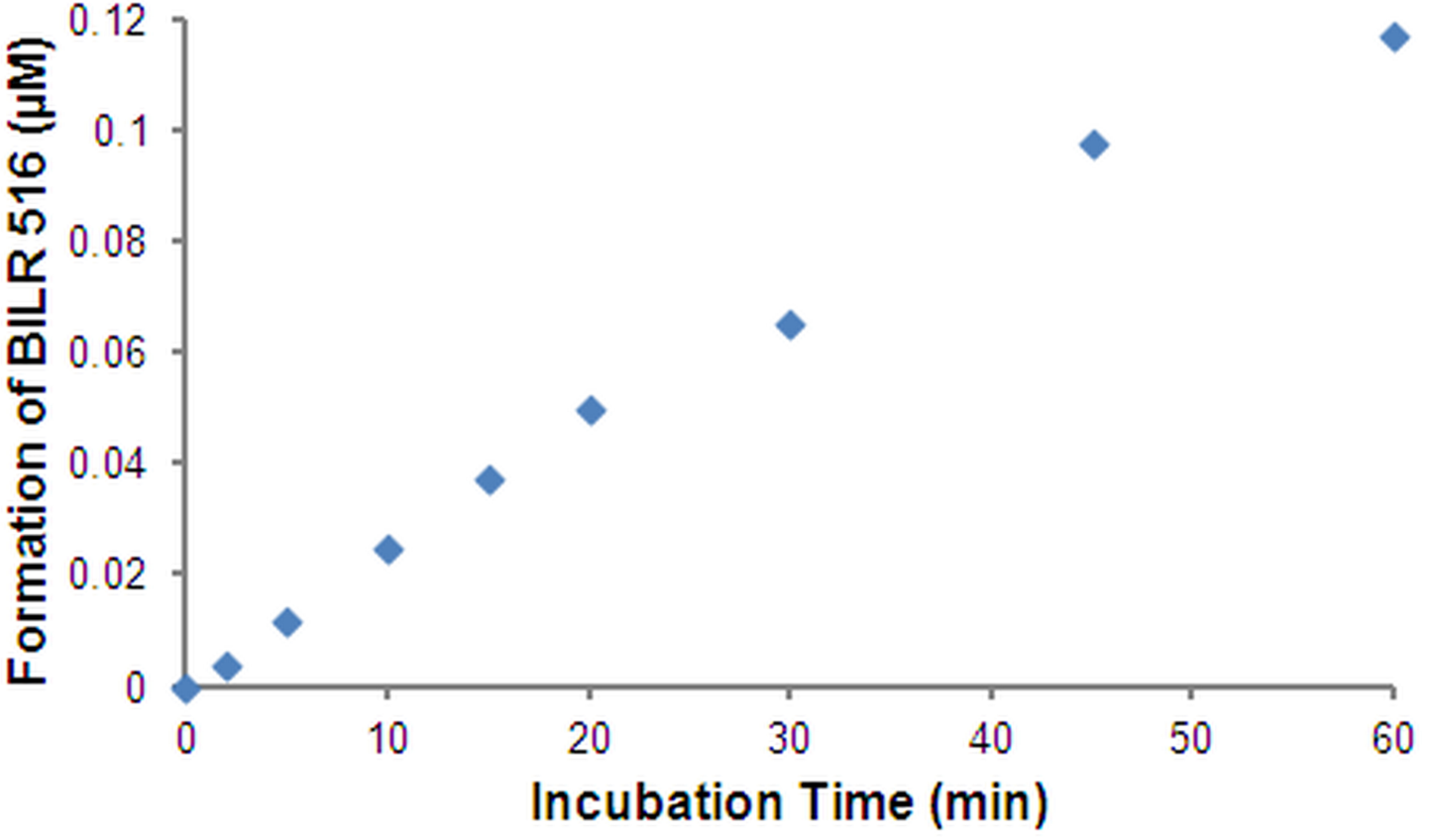
Formation of BILR 516 (µM)
0.12
0.1
0.08
0.06
0.04
0.02
0
0
10
20
30
40
50
60
Incubation Time (min)

Fig. 5

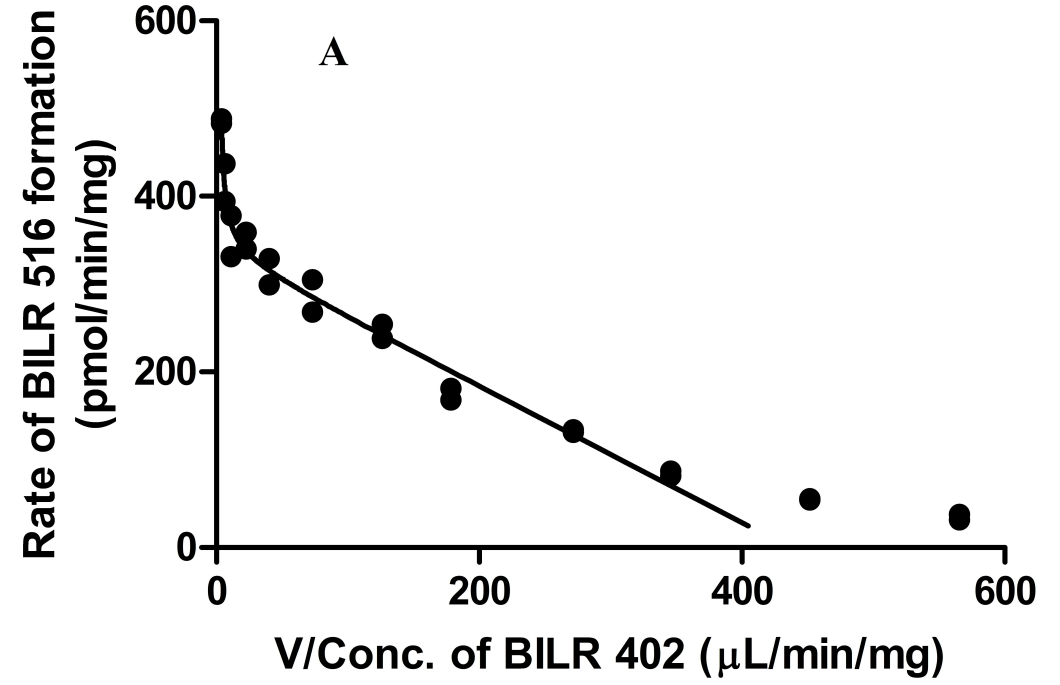
A
Rate of BILR 516 formation (pmol/min/mg)
600
400
200
0
0
200
400
600
V/Conc. of BILR 402 (μL/min/mg)

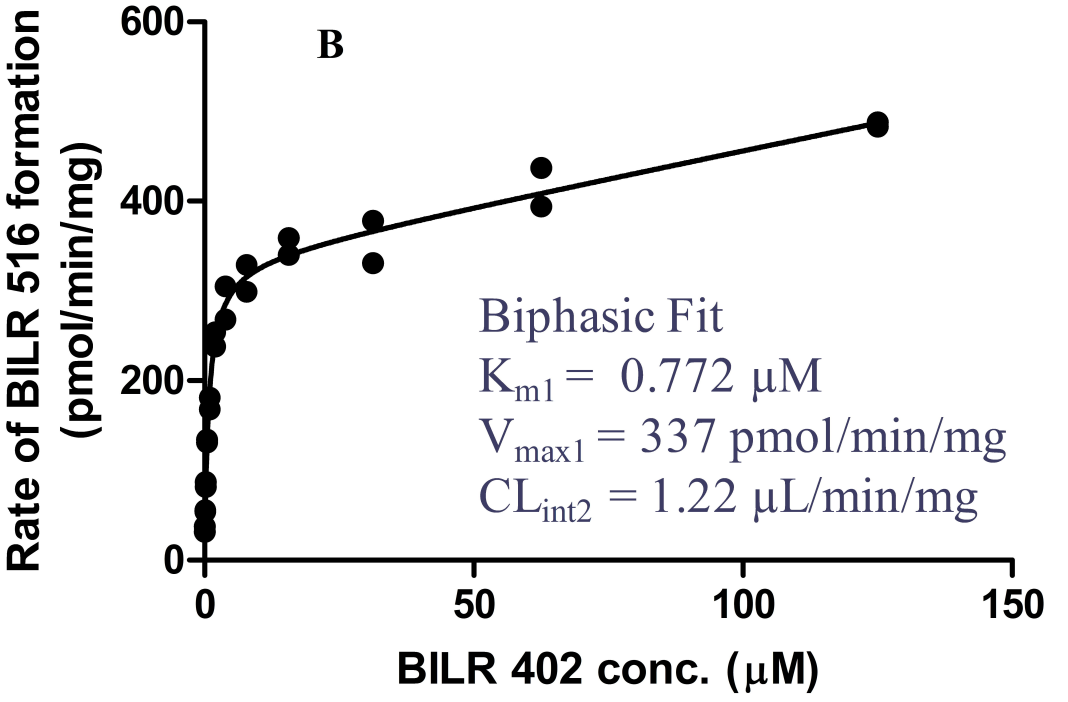
B
Rate of BILR 516 formation (pmol/min/mg)
600
400
200
0
0
50
100
150
BILR 402 conc. (μM)
Biphasic Fit
K_{m1} = 0.772 μM
V_{max1} = 337 pmol/min/mg
CL_{int2} = 1.22 μL/min/mg

Fig. 6

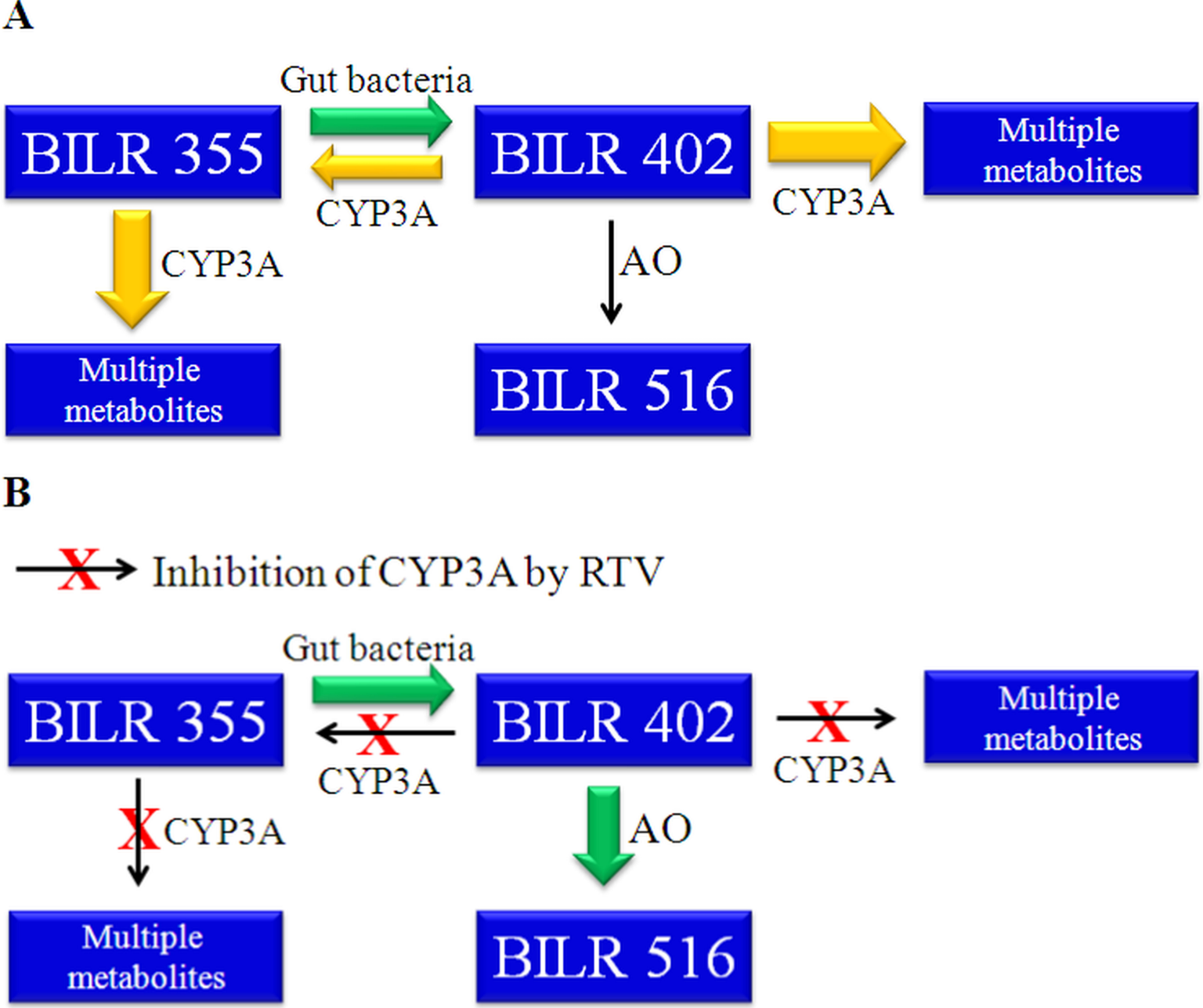
A
Gut bacteria
BILR 355
BILR 402
Multiple metabolites
CYP3A
CYP3A
CYP3A
AO
Multiple metabolites
BILR 516
B
Inhibition of CYP3A by RTV
Gut bacteria
BILR 355
BILR 402
Multiple metabolites
CYP3A
CYP3A
CYP3A
AO
Multiple metabolites
BILR 516

Fig. 7